
**Cansmart 2009**

*International Workshop*

**SMART MATERIALS AND STRUCTURES**

22 - 23 October 2009, Montreal, Quebec, Canada

# INTELLIGENT CONTROLLER FOR SMART BASE ISOLATION OF MASONRY STRUCTURES

S. Laflamme[1], T.-Y. Yu[2] and J. J. Connor[3]

[1]Deptartment of Civil and Environmental Engineering, Massachusetts Institute of Technology
laflamme@mit.edu
[2]Deptartment of Civil and Environmental Engineering, University of Massachusetts Lowell
TzuYang_Yu@uml.edu
[3]Deptartment of Civil and Environmental Engineering, Massachusetts Institute of Technology
jjconnor@mit.edu

## ABSTRACT

In this paper, an intelligent controller to control a smart base-isolated masonry structure is proposed. The smart base isolation consists of rubber bearings and a magnetorheological damper. This semi-active scheme takes advantage of the low power requirement of magnetorheological devices to achieve structural control.

The controller is capable of mapping the behaviour of the controlled structure sequentially, using a self-organizing neural network which has time-varying learning rates. This neurocontroller is augmented by a sliding mode controller to account for the uncertainty on the semi-active damping forces. Wavelets are used as functions in the single hidden layer for their capability of localizing functions in the space and frequency domains.

Results show that the intelligent controller is capable of rapidly mapping the inverse state-force relationship, without any prior knowledge of the dynamic properties of the controlled structure. The displacement control performance is similar to the performance from an active hybrid strategy, and the inter-story displacement is efficiently minimized.

***Keywords:*** Neurocontroller, magnetorheological dampers, adaptive control, intelligent control, civil structures, base isolation

## INTRODUCTION

In North America including Canada, a large number of historical buildings are unreinforced masonry or brick masonry. Without the presence of reinforcement in these structures, brittle

behaviours are to be expected in extreme loading events such as earthquakes. Such brittle behaviours are typically associated with significant economic and fatal losses. The heterogeneity and anisotropy of masonry structures also complicate the prediction of their mechanical behaviour in different stress states. Numerical modeling of masonry structures at micro- [1-2], meso- [3], and macro- [4-5] levels, as well as experimental investigation [6-9], have been reported in the literature. Failures of masonry structures can be attributed to various causes including lack of anchorage, anchor failure, in-plane failures, out-of-plane failures, combined in-plane and out-of-plane effects, and diaphragm-related failures [10]. These causes represent the low-ductility characteristic of masonry structures, leading to the vulnerability of masonry structures in seismic events.

Base isolation is a well understood technique often used to improve the performance of masonry structures for earthquake loadings. Base isolation is traditionally performed using a rolling pendulum system or lead-rubber bearings (LRB). The rolling pendulum system is known to be more cost effective than the LRB system, but has the disadvantage of a potential roll-off over large displacements [11]. Alhan and Gavin [12] surveyed research on control and uncontrolled base isolation systems, and noted that the addition of a passive system can significantly improve the performance of base isolation. Active systems can outperform passive systems, and their cost can be justifiable over a long period of control [13]. Semi-active systems, on the other hand, require little power and their performance is comparable to the performance of active systems. For this reason, the controlled system this paper is a base isolation system equipped with a magnetorheological (MR) damper. The main advantage of the hybrid semi-active system is the exclusion of the hysteretic material in the rubber bearing, which eliminates replacement cost and inoperability period associated with plastic deformation of the LRB system resulting from an earthquake. This strategy has been studied in the [11, 14]. This paper focuses on the on the semi-active controller of the smart base isolation strategy.

Application of semi-active and active control schemes to civil engineering structures is impeded by the inherent size of plants to be controlled. Three main control obstacles are specific to the field of civil engineering: 1) large actuating forces required; 2) uncertainties in dynamic characteristics; and 3) limited state measurements [15]. The use of semi-active devices, such as MR dampers, has been proposed for control of civil structures because of their capability to perform almost as well as active control schemes for mitigation of natural hazards, while requiring only a fraction of the power input [16-17]. The problem of uncertain dynamic properties and limited state measurement are more of a control and system identification issue. The use of adaptive controllers is therefore recommended.

Several adaptive controllers have been studied for control of civil structures. Robust controllers capable of performing despite system uncertainties, such as sliding mode control [18] and adapted LQR/$H_2$ control [19], have been proposed but the performance of such controllers is dependent on the initial estimation of the system properties. Neurocontrollers have also been proposed because of their capability to map nonlinear complex functions. Sanner and Slotine [20] were the first to use Gaussian radial functions for active control of nonlinear systems. Cannon and Slotine [21] proposed to use adaptive wavelets for neurocontrol.

Some applications of neurocontrol to civil structures have been recently studied, and are reviewed in [22]. This paper presents an adaptive neurocontroller for the application to a hybrid MR-base isolation system for masonry structures. The controller is a modification of prior work from the authors to provide enhanced robustness, as well as better space and frequency localization of the controlled plant. Its performance for a near-field type earthquake is assessed. This proposed controller has the unique characteristics of sequential learning and adaptive learning rates based on Lyapunov stability theory that are capable of accelerating convergence during high magnitude excitations. The applicability of this type of neurocontroller to large-scale civil structures is discussed in [22].

The paper is organized as follows: section 2 discusses MR dampers; section 3 presents the neurocontroller; section 4 describes the simulation; section 5 presents and discusses the results; section 6 concludes the paper.

## MAGNETORHEOLOGICAL DAMPERS

The application of MR dampers for control of civil structures has attracted some attention in the research community since the 1990's. Their low power requirement, along with their mechanical robustness and fail-safe property make them excellent candidate for vibration mitigation of large-scale systems. MR dampers are capable of generating a reaction force of 200 kN in 60 milliseconds, with a 50 W power input [23].

The mathematical complexity of MR dampers renders complicated the mapping of the required voltage for a desired force [24]. Some non-mathematical models have been developed, such as adaptive identification [25]. Despite that those models could be used with sequential learning, the use of the clipped-optimal algorithm proposed in Dyke et al. [26] has shown excellent performance and simplicity [16,27]. This scheme is used for the neurocontroller.

Because of the inherent state-dependence of the semi-active device, the required force by the proposed neurocontroller will not necessarily be achieved by the MR damper. There will be an error $\tilde{u}$ arising from the difference between the required force $u$ and the actual force $u_{act}$:

$$\tilde{u} = u - u_{act} \tag{1}$$

This error on the force is treated as a system uncertainty and is handled using a sliding mode controller described in the next section.

## CONTROLLER

The proposed controller is a modification of the controller presented in [22]. The robustness of the controller is significantly enhanced by the incorporation of a smooth interpolation between the required weight and the actual weight of a newly added node. Also, the functions of the neurocontroller are changed to "mexican hat" wavelets for their better space and frequency localization property, based on the work of Cannon and Slotine [21]. For completeness, the neurocontroller algorithm is fully described in this section.

Neurocontroller Architecture

The controller is a self-organizing single layer neural net comprising mexican hat wavelets $\phi$ of the form:

$$\phi(x) = \left(1 - \frac{\|x-\mu\|^2}{\sigma^2}\right) e^{\frac{-\|x-\mu\|^2}{\sigma^2}} \tag{2}$$

where $x$ is the input, $\mu$ and $\sigma$ are the center and bandwidth of the function respectively. Fig. 1 illustrates the mexican hat wavelet.

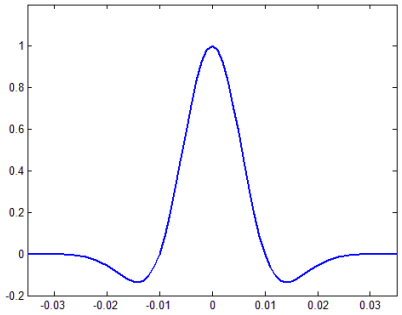


**Fig. 1**: Mexican hat wavelet; $\mu = 0$ and $\sigma = 0.01$.

The goal of the neurocontroller is to map the relationship control-input/state-output of the hybrid system. The network output, which is the required force $u$, can be written:

$$u_j(x) = \sum_{i=1}^{h} \alpha_{i,j}\, \phi_{i,j}(x) = \alpha_j^T \phi(x) \tag{3}$$

where $\alpha$ is the nodal weight associated with the output $j$. For simplicity, the neurocontroller will be presented for the case of a single actuator. The subscript $j$ will be dropped.

The self-organizing feature of the neurocontroller consists of adding a node when the Euclidian distance of a new output to the closest node is farther than the threshold $\lambda$. The network also has the capacity to prune nodes when their weights are found to be under a predefined ratio of the largest weight for several consecutive time steps. New nodes are added at the center of the new input, with the target weight $\alpha_T$ in function of the network error, while the bandwidth is computed based on the designed network density $\lambda$. Weights, centers and bandwidths are adaptive, and their adaptation rules are derived in the next subsection.

Adaptation Rules

Based on (3), the desired (optima) force $u_d$ from the network is written:

$$u_d = \alpha^T \phi(x) \tag{4}$$

Using (4) and the conventional state-space representation of the equation of motion of a civil structure, the dynamics of the controlled state error can be written as:

$$\dot{e} = \dot{X} - \dot{X}_d = Ae + B(u_{act} - u_d + \epsilon) = Ae + B\left(\hat{\alpha}^T\hat{\phi} - \alpha^T\phi - \tilde{u} + \epsilon\right) \tag{5}$$

where $X$ is the system state vector, $A$, $B$, and $u$ are notations that conform to the traditional state-space representation, the subscript $d$ denotes the desired states, the hat denotes estimated values, and $\epsilon$ is the estimation error. A sliding mode controller is used along with the following sliding surface as:

$$s = Pe \tag{6}$$

where the targeted surface is $s = 0$, $P$ is a user-defined vector that can be designed following [28]. Introducing the following control law:

$$u_{act} = \hat{\alpha}^T\hat{\phi} - k\big(\text{sign}(s)\big) \tag{7}$$

where $k$ is a constant to be defined later, (5) becomes:

$$\dot{e} = Ae + B\left(\hat{\alpha}^T\hat{\phi} - \alpha^T\phi - \tilde{u} + \epsilon - k\big(\text{sign}(s)\big)\right) \tag{8}$$

In order to find adaptation laws that would guarantee the stability of the wavelet network, Lyapunov theory is applied. Consider the following Lyapunov candidate:

$$V = \frac{1}{2}\left[s^Ts + \tilde{\alpha}^T\Gamma_\alpha^{-1}\tilde{\alpha} + \tilde{\phi}^T\Gamma_\phi^{-1}\tilde{\phi}\right] \tag{9}$$

where $\Gamma_\alpha^{-1}$ and $\Gamma_\phi^{-1}$ are positive definite diagonal matrices representing learning parameters, the tilde denotes the error between the estimated and real values ($\tilde{\alpha} = \hat{\alpha} - \alpha; \tilde{\phi} = \hat{\phi} - \phi$). Note that here $s$ is a scalar. Neglecting the higher order term, the time derivative of $V$ is:

$$\begin{aligned}\dot{V} &= s^TPAe + s^TPB\left(\hat{\alpha}^T\tilde{\phi} + \tilde{\alpha}^T\hat{\phi}\right) + \tilde{\alpha}^T\Gamma_\alpha^{-1}\dot{\hat{\alpha}} + \tilde{\phi}^T\Gamma_\phi^{-1}\dot{\tilde{\phi}} + \tilde{\alpha}^T\dot{\Gamma}_\alpha^{-1}\tilde{\alpha} \\ &\quad + \tilde{\phi}^T\dot{\Gamma}_\phi^{-1}\tilde{\phi} + s^TPB\epsilon - s^TPB\tilde{u} - |s^T|PBk \\ \dot{V} &= e^TP^TPAe + \tilde{\phi}^T\left(\hat{\alpha}^TB^TP^Ts + \Gamma_\phi^{-1}\dot{\tilde{\phi}}\right) + \tilde{\alpha}^T\left(\hat{\phi}^TB^TP^Ts + \Gamma_\alpha^{-1}\dot{\hat{\alpha}}\right) \\ &\quad - s^TPB(\tilde{u} - \epsilon) - |s^T|PBk + \tilde{\xi}^T\dot{\Gamma}^{-1}\tilde{\xi} - \tilde{\phi}^T\Gamma_\phi^{-1}\dot{\phi}\end{aligned} \tag{10}$$

with:

$$\tilde{\xi} = \begin{bmatrix}\tilde{\alpha} \\ \tilde{\phi}\end{bmatrix}, \Gamma = \begin{bmatrix}\Gamma_\alpha & 0 \\ 0 & \Gamma_\phi\end{bmatrix}$$

The tilde denotes the error between the optimal and current parameters. By choosing the following adaptation laws:

$$\dot{\hat{\alpha}} = -\left(\Gamma_\alpha \hat{\phi}\right) B^T P^T s \qquad (11)$$
$$\dot{\hat{\phi}} = -\left(\Gamma_\phi \hat{\alpha}\right) B^T P^T s$$
$$\dot{\Gamma}^{-1} = -s^T s I$$

where $I$ is an identity matrix to populate $\dot{\Gamma}^{-1}$, equation (10) becomes:

$$\dot{V} = e^T P^T P A e - s^T P B(\tilde{u} - \epsilon) - |s^T| P B k - \tilde{\xi}^T (s^T s I)\tilde{\xi} - \tilde{\phi}^T \Gamma_\phi^{-1} \dot{\phi} \qquad (12)$$

In the discrete form, the adaptation laws for $\mu$ and $\sigma$ are obtained by taking the partial derivatives of $\phi$. Choosing $k = \eta u_b$, where $\eta$ is positive, and $u_b$ is a known bound (also positive) on $\tilde{u}$, (12) can be rewritten as:

$$\dot{V} = e^T P^T P A e - s^T P B(\tilde{u} - \epsilon) - |s^T| P B \eta u_b - \tilde{\xi}^T (s^T s I)\tilde{\xi} - \tilde{\phi}^T \Gamma_\phi^{-1} \dot{\phi} \qquad (13)$$

where the term $k$ depends on the uncertainty on the error defined in (1). This error can be quite large, and increasing its value too much would lead to a controller based almost exclusively on the sign of the sliding surface. Instead, a bound $u_b$ is assumed, and adaptation on the network stopped when $|\tilde{u}| > u_b$. Each term of equation (13) can be shown to be at least negative semi-definite, except for the last term. Furthermore, as discussed previously, a smooth interpolation is incorporated when nodes are added to ensure the smoothness of the Lyapunov function (9):

$$\dot{\hat{\alpha}} = \begin{cases} -(\Gamma_\alpha \hat{\phi}) B^T P^T s & \text{if the node reached } \alpha_T \\ m(t)\alpha_T & \text{if the node was added but has not reached } \alpha_T \\ 0 & \text{if the node is added} \end{cases} \qquad (14)$$

with $m(t)$ being an infinitely differentiable function such as the sigmoid function.

## SIMULATION

A simulation has been done on a three degrees-of-freedom system used in previous work [23,27]. The stiffness at the base has been reduced by 40% to model a base isolation system consisting of rubber bearing. A 1100 N MR damper is attached between the ground slab and the first floor. Structural properties are as follows:

$$M = \begin{bmatrix} 98.3 & 0 & 0 \\ 0 & 98.3 & 0 \\ 0 & 0 & 98.3 \end{bmatrix} \text{kg}; \quad C = \begin{bmatrix} 175 & -50 & 0 \\ -50 & 100 & -50 \\ 0 & -50 & 50 \end{bmatrix} \frac{\text{N} \cdot \text{s}}{\text{m}}; \quad K = 10^5 \begin{bmatrix} 7.2 & -6.84 & 0 \\ -6.84 & 13.7 & -6.84 \\ 0 & -6.84 & 6.84 \end{bmatrix} \frac{\text{N}}{\text{m}}$$

To evaluate the performance of the controller, the simulation subjected the structure to the ElCentro 1940 earthquake, North-South component. This earthquake is a near-field type, and has the possibility to provoke a roll-off of the structure. The time scale of the earthquakes has been scaled by a factor of five to take into consideration the model sizing. The neurocontroller uses displacement and velocity inputs, along with the previous applied forced. Because large displacements are the main cause of structural failures during an earthquake, the dynamic

outputs to be controlled are the floor displacements. Results are shown and compared in the next section.

## RESULTS

The network parameters quickly converge when the neurocontroller uses an actuator, but the convergence rate is slower when the MR damper is used, as expected. Fig. 2 shows the time series plots obtained from the simulation. Fig. 2a) compares the performance of the controller using the MR device to the performance of the same controller using an actuator. Results show that the performance of an MR damper is similar to the performance of an actuator. Fig. 2b) shows the time series results for the semi-active controller along with the passive-on and passive-off cases. Passive-off refers to the MR damper with no current input, while the passive-on refers to the MR damper with full current input. In addition to the advantage of saving power, the semi-active control strategy appears to be more efficient at mitigating the 3rd floor displacement.

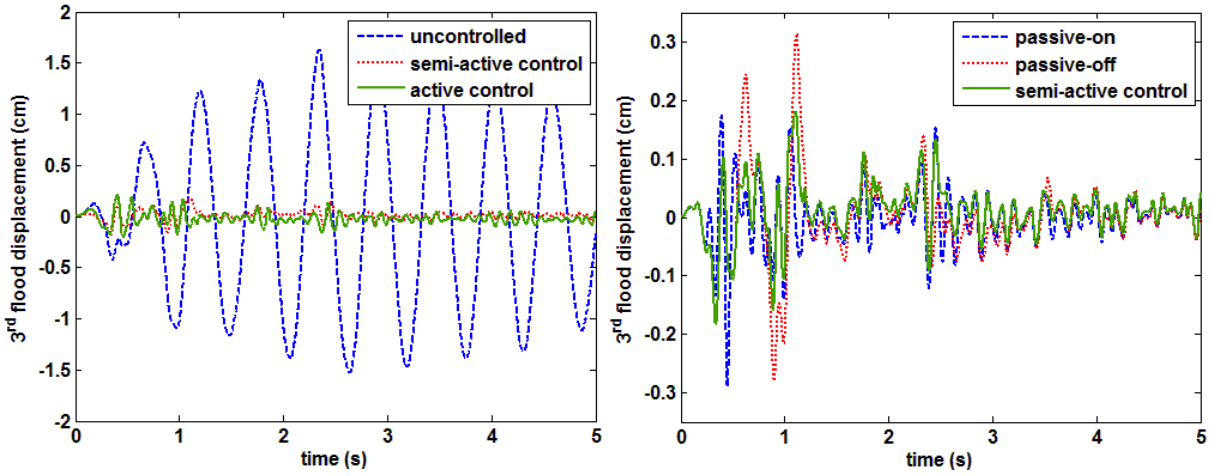


(a) (b)

**Fig. 2**: 3rd floor displacements for El Centro earthquake;
a) uncontrolled case compared to semi-active and active control strategies
b) semi-active control strategy compared to passive-on and passive-off cases

Fig. 3 compares the inter-story displacements of various control strategies. It is observed that the semi-active controller is capable of keeping a minimal inter-story displacement, while limiting the displacement at the first floor. The passive-on case gives the best performance at mitigating the first floor displacement as it is equivalent to locking the floor, but this is done at the expense of larger inter-story displacements, meaning that the advantage of base isolation is cancelled.

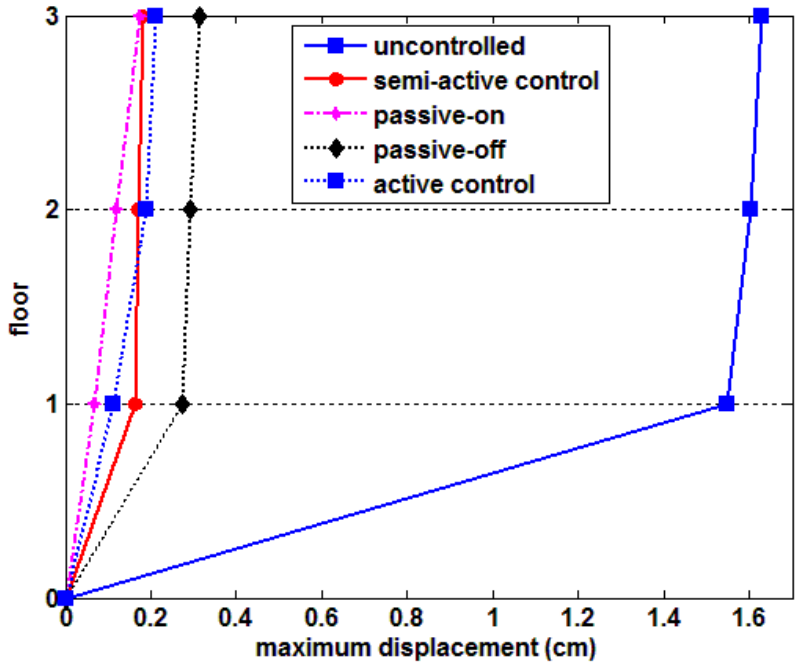


**Fig. 3**: Maximum floor displacement for each strategy

Table 1 summarizes the displacement reductions for various control strategies. The linear quadratic regulator (LQR) optimal controller is designed using full knowledge of the plant for comparison purposes. The semi-active control strategy shows comparable performance with the active case.

| | Passive-on | Passive-off | Semi-active control | Active control | LQR control |
|---|---|---|---|---|---|
| 1st floor | 93.6% | 82.3% | 89.4% | 92.7% | 92.9% |
| 2nd floor | 88.4% | 81.7% | 89.2% | 88.2% | 92.4% |
| 3rd floor | 82.3% | 80.7% | 88.8% | 87.1% | 88.3% |
| max damping force (N) | 982 | 211 | 731 | 1100 | 1100 |

**Table 1**: Summary of displacement reductions for each strategy.

Table 2 summarizes the performance of the neurocontroller with different inputs. The proposed neurocontroller uses displacement and velocity feedback, but its performance has been studied for the case of pure acceleration feedback. Notice that acceleration feedback would normally prevent the use of an adaptive observer or numerous sensors, but since the neurocontroller uses a sliding mode control scheme, displacement and velocity measurements will be needed to compute the sliding surface. The importance of carefully choosing the network inputs is highlighted in this analysis.

| | displacement 1st floor | displacement 2nd floor | displacement 3rd floor | maximum damping force |
|---|---|---|---|---|
| displacement and velocity feedback | 0.164 | 0.173 | 0.182 | 731 |
| pure acceleration feedback | 0.178 | 0.206 | 0.235 | 740 |
| relative change | 8.5% | 19% | 29% | 1.2% |

**Table 2**: Comparison of displacement/velocity feedback with acceleration feedback

## CONCLUSION

From the simulation and analysis results provided in this paper, it is found that the proposed neurocontroller provides good performance for controlling the base displacement of a smart base isolation scheme by efficiently minimizing the inter-story displacements. Its performance is similar to the active case, and the displacement shape of the uncontrolled case is preserved. Current work is undergoing at MIT to formalize the type of inputs that can optimize the architecture of the neurocontroller.

## REFERENCES


1. Lourenco, P. B., and Rots, J. G.(1997), "A multisurface interface model for analysis of masonry structures," J Eng Mech, ASCE, 123(7): 660-668.
2. Zucchini, A., and Lourenco, P.B. (2007), "Mechanics of masonry in compression: Results from a homogenization approach," Computer and Structures, 85: 193-204.
3. Sheieh-Beygi, B, and S Pietruszczak (2008), "Numerical analysis of structural masonry: mesoscale approach," Computers and Structures, 86: 1958-1973.
4. Hamid, A. A., and Drysdale, R. G. (1981), "Proposed failure criteria for concrete block masonry under biaxial stress," J Struct Div, ASCE, 107(8): 1675-1687.
5. El-Dakhakhni, W. W., Drysdale, R. G., and Khattab, M. M. (2006), "Multilaminate macromodel for concrete masonry: Formulation and verification," J Struct Eng, ASCE, 132 (12): 1984-1996.
6. McNary, W. S., and Abrams, D. P. (1985), "Mechanics of masonry in compression," J Struct Eng, ASCE, 111(4): 857-870.
7. Atkinson, R. H., Noland, J. L., Abrams, D. P.,and McNary, S. (1985), "A deformation failure theory for stack-bond masonry prisms in compression," Proc. 3rd North American Masonry Conf, Arlington, TX: 18-1-18.
8. Pluijm, R. van der (1992), "Material properties of masonry and its components under tension and shear," Proc. 6th Canadian Masonry Symp, by VV Neis (ed.), Saskatchewan, Canada: 675-686.
9. Syrmakezis, C. A., and Asteris, P. G. (2001), "Masonry failure criterion under biaxial stress state," J Mat in Civil Eng, ASCE, 13(1): 58-64.
10. Burneau, M. (1994), "State-of-the-art report on seismic performance of unreinforced masonry buildings," J Struct Eng, ASCE, 120 (1): 230-251.
11. Shook, D., Lin, P.-Y., Lin, T.-K., & Roschke, P. N. (2007). "A Comparative Study in the Semi-Active Control of Isolated Structures", Smart Mat and Struct, 16, 1433-1446.

12. Alhan, C., & Gavin, H. P. (2005). "Reliability of base isolation for the protection of critical equipment from earthquake hazards", Engineering Structures, 27, 1435-1449.
13. Wen, Y. K., & Shinozuka, M. (1998), "Cost-Effectiveness in Active Structural Control", Engineering Structures , 20 (3), 216-221.
14. Zhou, L., Chang, C.-C., & Wang, L.-X. (2003), "Adaptive Fuzzy Control for Nonlinear Building-Magnetorheological Damper System", J Struct Eng, 905-913.
15. Burdisso, R. A. (1994), "Structural Attenuation due to Seismic Inputs with Active/Adaptive Systems", Proc. First World Conference on Structural Control, Los Angeles, California, (TA4), 3-12.
16. Jansen, L. M., & Dyke, S. J. (2000), "Semiactive Control Strategy for MR Dampers: Comparative Study", Journal of Engineering Mechanics, 126 (8), 795-803.
17. Spencer, B. F., Dyke, S. J., Sain, M. K., & Carlson, J. D. (1997), "Phenomenological Model for Magnetorheological Dampers", J of Eng Mechanics, 123 (33), 230-238.
18. Yang, J. N., Wu, J. C., & Agrawal, A. K. (1995), "Sliding Mode Control for Nonlinear and Hsteretic Structures", Journal of Engineering Mechanics, 121 (12), 1330-1339.
19. Wang, S.-G., Yeh, H. Y., & Roschke, P. N. (2001, June 25-27), "Robust Control for Structural Systems with Parametric and Unstructured Uncertainties", Proc. American Control Conference, 1109-1114.
20. Sanner, R., & Slotine, J.-J. (1992), "Gaussian Networks for Direct Adaptive Control", IEEE Transaction on Neural Networks, 3 (6), 837-863.
21. Cannon, M., & Slotine, J.-J. E. (1995), "Space-Frequency Localized Basis Function Networks for Nonlinear System Estimation and Control", Neurocomputing, 9, 293-342.
22. Laflamme, S. & Connor, J. (2009), "Application of Self-Tuning Gaussian Networks for Control of Civil Structures Equipped with Magnetorheological Dampers", Proc. of SPIE Smart Structures and Materials & NDE and Health Monitoring, 7288, 1-12.
23. Yang, G., Spencer, B. J., Jung, H.-J., & Carlson, J. (2002), "Large-Scale MR Fluid Dampers: Modeling and Dynamic Performance Considerations", Engineering Structures (24), 309-323.
24. Li, H.-N., & Chang, Z.-G. (2008), "Semi-Active Control for Eccentric Structures with MR Damper Based on Hybrid Intelligent Algorithm", Structural Design of Tall and Special Buildings, 17 (1), 167-280.
25. Terasawa, T., Sakai, C., Ohmori, H., & Sano, A. (2004), "Adaptive Identification of MR Damper for Vibration Control", 43rd IEEE Conf on Decision and Control, 2297-2303.
26. Dyke, S., Spencer, B., Sain, M., & Carlson, J. (1996), "Modeling and Control of Magnetorheological Dampers for Seismic Response Reduction", Smart Materials and Structures, 5 (5), 565-575.
27. Yoshida, O., Dyke, S. J., Giacosa, L. M., & Truman, K. Z. (2003), "Experimental Verification of Torsional Response Control of Asymetric Buildings using MR Dampers", Earthquake Engineering and Structural Dynamics, 32 (13), 2085-2105.
28. Utkin, V. I., & Yang, K. D. (1978), "Methods for Constructing Discontinuity Planes in Multidimensional Variable Structure Systems", Autom Remote Control , 39 (10), 1466-1470.